Colloid Polym Sci (2007) 285:1433–1439
DOI 10.1007/s00396-007-1700-2

ORIGINAL CONTRIBUTION

Thermoresponsive polymeric nanoparticles stabilized by surfactants

Čestmír Koňák · Jiří Pánek · Martin Hrubý

Received: 11 April 2007 / Accepted: 16 May 2007 / Published online: 7 June 2007

Abstract Solutions of poly(*N*-isopropylacrylamide) (PNIPA) with ionic and nonionic surfactants were investigated by light scattering methods at temperatures 15–45 °C. In contrast to previous studies, where surfactants were used in excess, lower concentrations of surfactants were used. The formation of well-defined nanoparticles of PNIPA was observed on heating above the lower critical solution temperature. The effect of PNIPA and surfactant concentrations, and molecular weight of PNIPA on nanoparticle parameters and on the phase transition temperature of PNIPA solutions were investigated. An interpretation based on stabilization of PNIPA nuclei by surfactants was suggested.

Keywords Light scattering · Nanoparticles · Particle nucleation · Poly(*N*-isopropylacrylamide) · Surfactants

Introduction

In the past decade, stimuli-responsive polymers that change their properties in a desired way responding to a small change in temperature, pH, electric or magnetic field, or other parameters attracted much attention [1–3]. Probably the most often studied polymer systems are those based on poly (*N*-isopropylacrylamide) (PNIPA) [4–6]. PNIPA undergoes a coil-to-globule transition at 32 °C (lower critical solution temperature, LCST [5]) close to physiological temperature, which makes the polymer an especially good candidate for applications in biotechnology and in medicine [1, 3, 7].

In our previous paper [8], aqueous solutions of poly (*N*-isopropylacrylamide) (PNIPA) and sodium dodecyl sulfate (SDS) mixtures were investigated by light scattering methods in the temperature region 15–40 °C. Unlike in previous studies [9, 10], lower concentrations of SDS were used. Under such conditions, PNIPA formed well-defined nanoparticles with molecular weights, M_w, from 1 to 10×10^7 and hydrodynamic radii, R_h, from 20 to 30 nm at 40 °C. Higher surfactant concentrations resulted in intermolecular solubilization of PNIPA above the LCST in agreement with published results [11–15].

The nanoparticle parameters can be varied by PNIPA and surfactant concentrations (c_{PNIPA} and c_{SDS}, respectively) and the viscosity-average molecular weight of PNIPA, M_η, in a wide range of M_w and R_h values. M_w and R_h of the resulting thermosensitive nanoparticles (at 40 °C) decreased with increasing concentration of SDS and of PNIPA, as well as with increasing viscosity-average molecular weight of PNIPA, M_η.

The observed formation of well-defined thermosensitive nanoparticles was qualitatively explained by stabilization of monodisperse nuclei of PNIPA with SDS in the transition region of phase separation of PNIPA. The adsorbed SDS hydrophilizes the nanoparticle surface. If the amount of adsorbed SDS reached the critical surface concentration, the nanoparticles are sufficiently solubilized and the growth of nanoparticles stopped.

In the present paper, the above mentioned investigation of nanoparticle formation in mixed SDS/PNIPA solutions is further extended to solutions of PNIPA with several ionic and nonionic surfactants (SR). Particularly the nanoparticles covered with block copolymer surfactants with soluble poly (oxyethylene) (PEG) blocks seem to be good candidates for applications in biotechnology and in medicine.

Č. Koňák (✉) · J. Pánek · M. Hrubý
Institute of Macromolecular Chemistry,
Academy of Sciences of the Czech Republic,
Heyrovsky Sq. 2,
162 06 Prague 6, Czech Republic
e-mail: konak@imc.cas.cz

Experimental part

Materials and methods

Linear PNIPA were purchased from Polymer Source Inc. Polymers with viscosity-average molecular weight M_η= 67,000, 122,000, and 220,000 were used for investigation.

Sodium dodecyl sulfate (SDS), 1-hexadecylpyridinium chloride monohydrate (HDPC), and Pluronic F-68 (PL) were obtained from Sigma, hexadecyltrimethylammonium bromide (CTAB), Brie 97 (B97) and 98 (B98) were from Aldrich. Q-water was used as a solvent.

Parameters of surfactants are given in Table 1.

We have used three ionic surfactants, two negatively charged and one positively charged, and three nonionic surfactants.

Preparation of nanoparticles

Nanoparticles were prepared by heating SR/PNIPA solutions above the LCST up to 40 °C.

Two procedures were used:

(a) The measurement cell with 1 ml of the solution was immersed into a stirred water bath at 40 °C. The transition region of PNIPA (32 °C) was reached in 40 s. The cell was then transferred to a preheated sample holder for measurements.
(b) Cell with the solution was inserted into Zetasizer at room temperature and heated (or cooled) in 1 °C steps up/down. On every temperature change, the measurements were performed after reaching the steady conditions, typically after 20 min in the phase separation region. On cooling, the light scattering data were taken after the fixed waiting time of 20 min.

Static and dynamic light scattering

Static light scattering (SLS) measurements were carried out with a home-made instrument equipped with a 30 mW He–Ne laser in the angular range 30–140° at temperatures from 25 to 40 °C. The SLS data were analyzed using the Zimm plot procedure. The data analysis based on a fit procedure by theoretical model curves in a scaled representation [16, 17] was used to obtain zero-angle values of apparent weight-average molecular weight M_{wa} and radius of gyration R_g. The concentration dependence was neglected, which seems to be justified because of low concentrations of the latex solutions (below 5×10^{-4} g·ml^{-1}). Thus, M_{wa} is a good approximation for the weight-average molecular weight M_w of nanoparticles at infinite dilution. The refractive index increment, dn/dc, of PNIPA (0.194 ml·g) was taken from literature [18].

Polarized dynamic light scattering measurements were made on the same instrument as SLS ones using an ALV 5000 multibit autocorrelator. The time autocorrelation functions were fitted assuming the Pearson distribution of characteristic relaxation times, τ_c [19, 20]:

$$z(\tau_c) = \tau_o^P \tau_c^{-p-1} \exp(-\tau_c/\tau_o)/\Gamma(p) \quad (1)$$

where τ_o and p are parameters, and $\Gamma(p)$ is the gamma function of parameter p. The average hydrodynamic radius, R_h, was calculated from the diffusion coefficient, using the Stokes-Einstein equation. The experimental error of the R_h determination was typically about 3%.

Temperature changes of the particle hydrodynamic radius, R_h, and scattering intensity, I_s, were automatically measured at the scattering angle 173° on a Nano-ZS, Model ZEN3600 (Malvern Instruments, UK) zetasizer. For evaluation of data, the DTS (Nano) program was used. The temperature dependences of I_s were used only for determination of the transition temperature, T_{tr}.

Results

In contrast to previous studies [9–14, 21–23], where the effect of ionic surfactants on the solubilization and conformations of PNIPA macromolecules was studied, the formation and properties of PNIPA nanoparticles stabilized by ionic and nonionic surfactants are investigated in the present study. In agreement with our previous paper [8],

Table 1 Parameters of surfactants used in the study

Surfactant	Code	CMC (mmol·l^{-1}]	CMC (mg·ml^{-1})	Mw (g·mol^{-1})	References
Sodium dodecyl sulfate	SDS	8.1	2.3	288.38	[15]
Cetyltrimethylammonium bromide	CTAB	1.00	0.387	384.44	[28]
Cetylpyridinium chloride	CPC	0.11	0.035	320.00	[29]
Pluronic F-68	F68	5.45	45.8	8 400	[30]
Polyoxyethylene(20) oleyl ether	Brie 98, B98	–	<0.025	1 150	LS[a]
Polyoxyethylene(10) oleyl ether	Brie 97, B97	–	<0.025	709	LS[a]

[a] Light scattering measurements

low concentrations of SR ($c_{SR} \leq 5 \times 10^{-4}$g · ml^{-1}) were used in this investigation. Under such conditions, the surfactants are not able to prevent intermolecular aggregation and well-defined nanoparticles of PNIPA are obtained above the LCST. This is demonstrated in Fig. 1 where the temperature dependence of the hydrodynamic radius, R_h, measured at θ=173° is shown for polymer concentration $c_{PNIPA} = 5 \times 10^{-4}$g · ml^{-1} and B98 concentration $c_{B98} = 5 \times 10^{-5}$g · ml^{-1}. M_η of the PNIPA used was 122,000.

The formation of nanoparticles starts in the vicinity of the critical solution temperature, 32 °C, which is manifested itself by an increase in R_h. In this study, we have defined the transition temperature, T_{tr}, as a temperature at which the volume fraction of nanoparticles for the first time exceeded the volume fraction of free PNIPA molecules upon heating of the investigated solution. Only R_h of the dominant component was plotted in Fig. 1. Consequently, R_h values of single molecules are presented for temperatures below T_{tr} while R_h of nanoparticles is used for temperatures above T_{tr}. The formation of nanoparticles was also accompanied by a sharp increase in I_s. The increase of R_h stopped above T_{tr} at about 100 nm. R_h of particles increases on cooling below the transition temperature reflecting swelling of particles before dissolution. Finally, the particles again dissolved. While the steady values of R_h obtained on heating were used for plotting Fig. 1, the R_h values measured on cooling were obtained after a fixed waiting time of 20 min. Since dissolution of nanoparticles on cooling is a slow process, 20 min was not sufficient for reaching steady conditions. Therefore, the observed hysteresis in Fig. 1 is partly due to kinetics of nanoparticle dissolution. The nanoparticles fully dissolve at 3 °C after 24 h and then the solution can be again used for further experiments.

The weight-average molecular weight, M_w, hydrodynamic radius, R_h, radius of gyration, R_g, and polydispersity of nanoparticles, $\Delta R_h/R_h$ (ΔR_h is the half-width of R_h-distribution at the half height) obtained at 40 °C (proce dure a) are shown for all the SR/PNIPA solutions used in the study in Table 2. Results for SDS/PNIPA solutions published in the previous paper [8] are used through the paper for comparison.

Well-defined nanoparticles were obtained in all the cases. The polydispersity of nanoparticles is low, ca. 0.1. R_h of nanoparticles in solutions with ionic surfactants is about 30 nm and M_w about 1.4×10^7. Larger particles were observed in solutions with nonionic surfactants: R_h with about 100 nm and M_w more than one order of magnitude higher than in solutions with ionic surfactants. The nanoparticles are stable for at least 24 h. The parameters are practically the same for both the preparation methods. The only difference between the results is the presence of a small amount of large aggregates in solutions prepared by slow heating. Reproducibility of preparation of nanoparticles was high in PNIPA solutions with ionic surfactants. R_h of nanoparticles varied only in percents. The reproducibility of R_h of nanoparticles prepared in PNIPA solutions with nonionic surfactants—ca. 10%—was worse than of those with ionic.

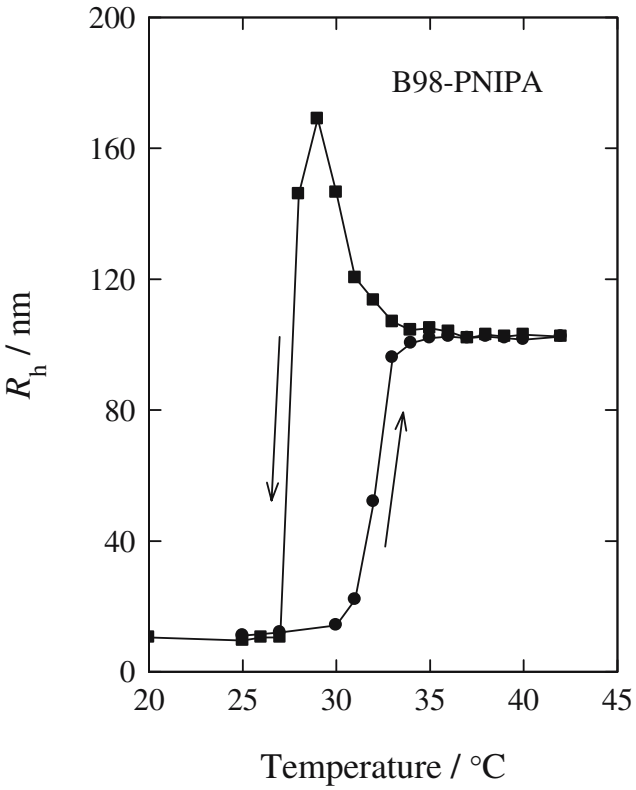

Fig. 1 Temperature dependence of the hydrodynamic radius, R_h, at θ=173°: (*filled circle*) measured on heating (procedure b), (*filled square*) slow stepwise cooling (procedure b) after fast heating of solution to 40 °C (procedure a). M_η=122,000, $c_{PNIPA}=5\times10^{-4}$ and $c_{B98} = 5 \times 10^{-5}$g · ml^{-1}

In contrast, the PNIPA solutions of the same concentration used without any surfactants are very turbid and slowly flocculate after heating above T_r.

The effect of CTAB concentration on the temperature dependence of I_s measured at the scattering angle θ=173° is shown for CTAB/PNIPA solutions with polymer concentration $c_{PNIPA} = 5 \times 10^{-4}$g · ml^{-1} in Fig. 2.

Table 2 Characteristics of nanoparticles (procedure a)

Surfactant	$M_w \times 10^{-6}$	R_g (nm)	R_h (nm)	$\Delta R_h/R_h$
SDS [8]	13	18	25	0.17
CTAB	14	20	27	0.15
HDPC	14	25	33	0.23
PL	640	78	100	0.09
B98	570	87	112	0.10
B97	880	116	136	0.09

M_η=122,000, $c_{PNIPA} = 5 \times 10^{-4}$ and $c_{SR} = 5 \times 10^{-5}$ g · ml^{-1}

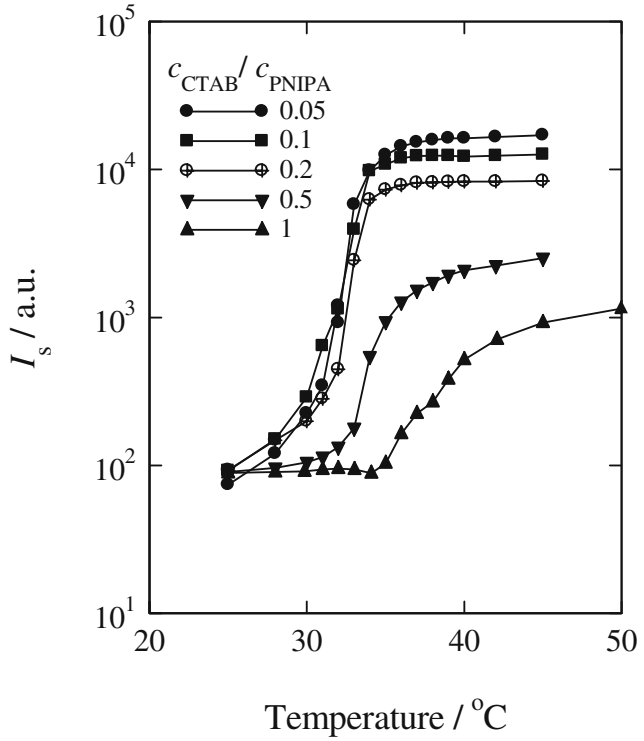

Fig. 2 Effect of relative CTAB concentration (c_{CTAB}/c_{PNIPA}) on the phase transition tested by scattered light intensity, I_s (procedure b). M_η=122,000, $c_{PNIPA} = 5 \times 10^{-4}$g · ml^{-1}

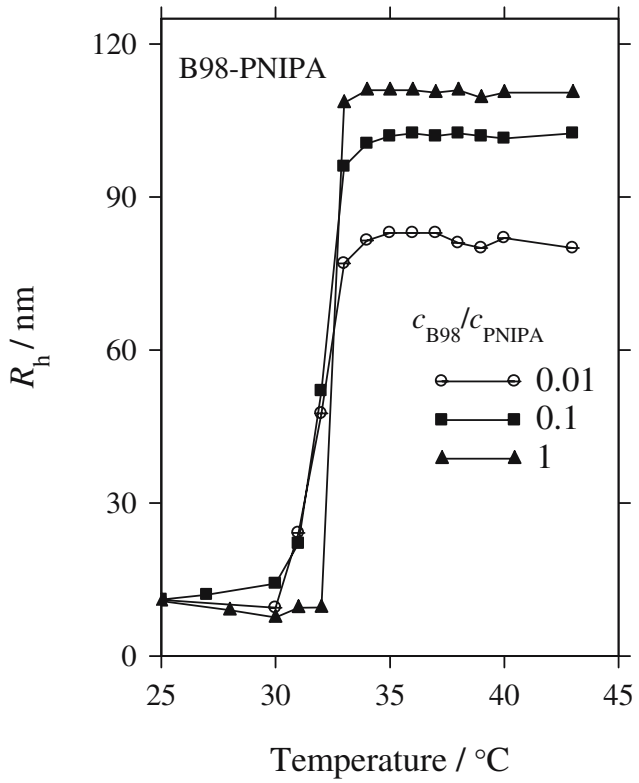

Fig. 3 Effect of relative B98 concentration (c_{B98}/c_{PNIPA}) on the phase transition tested by the hydrodynamic radius, R_h (procedure b). M_η= 122,000, $c_{PNIPA} = 2 \times 10^{-4}$g · ml^{-1}

The saturated values of I_s at temperatures above T_{tr} are lower for the solutions with high contents of CTAB (c_{CTAB}/c_{PNIPA}=1) than those for solutions with lower amounts of CTAB. Consequently, the M_w and R_h values of the resulting nanoparticles (at 40 °C) decrease with increasing value of the c_{SDS}/c_{PNIPA} ratio. Similar behavior was observed in SDS/PNIPA solutions [8]. The effect can be explained in accord with previously published results by the solubilization of PNIPA by the surfactant, which increases with increasing content of SDS [9–14, 21–23]. This manifests itself by suppression of intermolecular aggregation.

While M_w and R_h of nanoparticles decrease with increasing concentration of ionic surfactants, the opposite dependence was found for nonionic Brie 98 surfactants. This is demonstrated for B98/PNIPA solutions in Fig. 3, where temperature dependence of R_h is plotted for three c_{B98}/c_{PMIPA} ratios ($c_{PNIPA} = 2 \times 10^{-4}$g · ml^{-1}).

Light scattering results are collected in Fig. 4 where dependences of M_w and R_h values of nanoparticles on the c_{SR}/c_{PNIPA} ($c_{PNIPA} = 5 \times 10^{-4}$g · ml^{-1}) measured at 40 °C (procedure a) are shown for selected surfactants. SDS results are given for comparison. Both the particle parameters are practically independent of surfactant concentration for Pluronic F68 copolymer.

Also other parameters of ionic SR/PNIPA solutions are influenced by the surfactant content (see Fig. 5).

In contrast to nonionic surfactants, where transition temperature T_{tr} is practically independent of surfactant concentration (cf. Fig. 3), T_{tr} increases upon increasing the c_{SDS}/c_{PNIPA} ratio for ionic surfactants (Fig. 5). Polydispersity $\Delta R_h/R_h$ of nanoparticles, which is again practically independent of the surfactant concentration for nonionic surfactants, changes with SDS and CTAB concentration in a more complex way (see Fig. 5). The best nanoparticles with a polydispersity comparable with micelles were observed at c_{SR}/c_{PNIPA}=0.02 or 1 for both the surfactants.

The effect of PNIPA concentration on nanoparticle parameters (M_{wa} and R_h) is shown for solutions with the fixed c_{SDS}/c_{PNIPA}=0.1 in Fig. 6.

Again there is a difference in behavior between ionic and nonionic surfactants. While M_w and R_h decrease with increasing c_{PNIPA} for ionic surfactants, both the parameters increase for nonionic ones.

The effect of molecular weight of PNIPA on nanoparticle parameters is shown in Table 3.

It can be seen that M_w and R_h of particles decrease with increasing molecular weight of the polymer for three selected surfactants. This behavior is explained in Discussion.

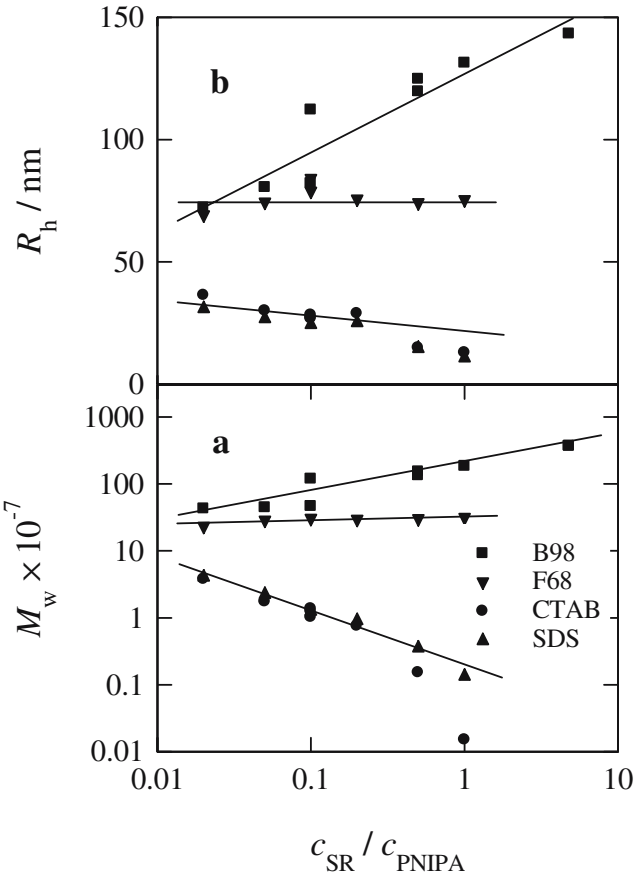

Fig. 4 Dependences of **a** molecular weight, M_{wa}, and **b** hydrodynamic radius, R_h, of nanoparticles on c_{SR}/c_{PNIPA} at 40 °C (procedure a). M_η=122,000, $c_{PNIPA} = 5 \times 10^{-4}$g · ml^{-1}

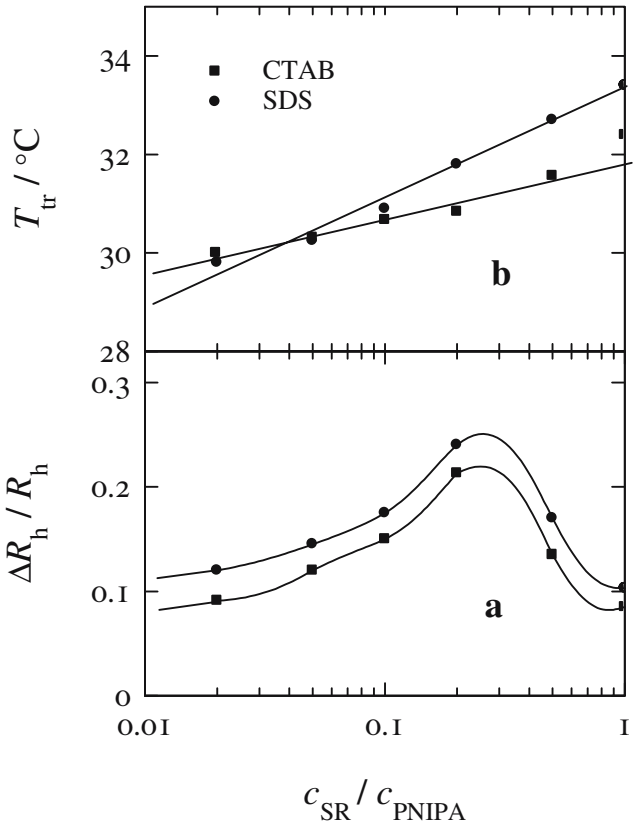

Fig. 5 Dependences of the **a** size polydispersity, $\Delta R_h/R_h$, and **b** transition temperature, T_{tr}, of nanoparticles on concentration of ionic surfactants (c_{SR}/c_{PNIPA}) at 40 °C (procedure a). M_η=122,000, $c_{PNIPA} = 5 \times 10^{-4}$g · ml^{-1}

Discussion

The observed formation of well-defined thermosensitive nanoparticles can be qualitatively explained by the model proposed in our previous paper [8]. The nuclei of a condensed phase formed after the polymer solution passes through the phase transition temperature are monodisperse at the early stage of phase separation [24, 25]. They are hydrophobic, and therefore, they attract surfactants molecules. If the adsorbed surfactant reaches a critical surface concentration, the nanoparticles are sufficiently solubilized, and the growth of nanoparticles stops.

Now, the effect of molecular weight of surfactants on the parameters of nanoparticles can be explained (Table 2). Diffusion of low-molecular-weight ionic surfactants is faster than that of nonionic ones. Ionic surfactants are able to stop the growth of nuclei earlier at lower values of M_w and R_h than nonionic ones.

The effect of molecular weight of the polymer on M_w and R_h of nanoparticles can be also explained. Note that the growth rate of nuclei is among others controlled by polymer diffusion. While the transport of surfactants is independent of molecular weight of the polymer, the growth rate of nuclei slows down with increasing molecular weight of the polymer. As a consequence, the growth of PNIPA nuclei stops with increasing surfactant sorption at smaller sizes for high M_η than at low ones. Therefore, M_{wa} and R_h of nanoparticles decrease with increasing M_η.

The effect of surfactant concentration can be also explained, at least for ionic surfactants. The higher is the concentration of ionic surfactants in solution the faster is reached their critical concentration on the nuclei surface and nucleation stops earlier at smaller values of M_{wa} and R_h. The problem of nonionic surfactants is more complex. While the ionic surfactant concentrations used in experiments are below CMC, the concentrations of B98 are still above the CMC (see Table 1). If we assume that copolymer micelles of the Brie copolymers are inactive in particle stabilization, the stabilization of nanoparticles is only dependent on the free surfactant concentration. The free surfactant (unimer) concentration increases with decreasing copolymer concentration on approaching CMC. It is probably a reason why the opposite behavior was observed.

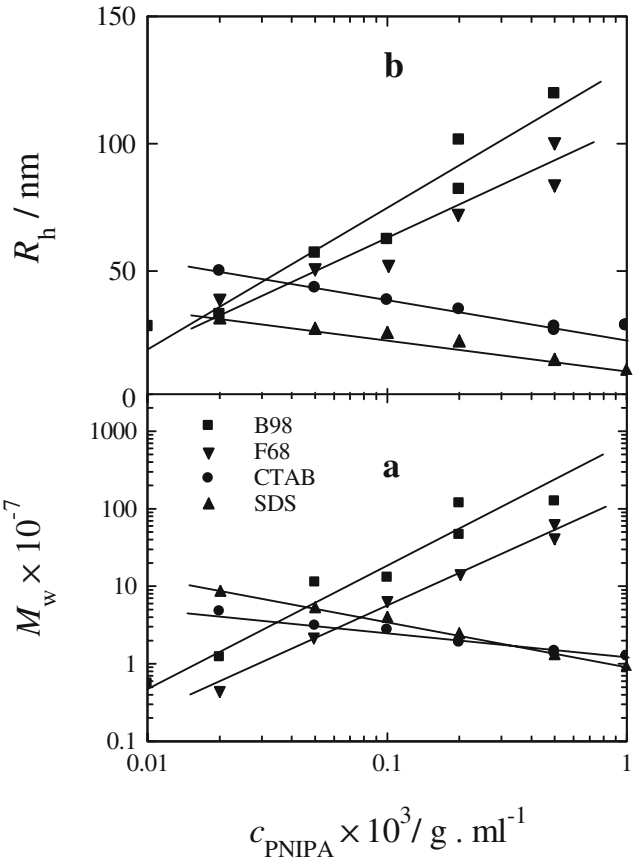

Fig. 6 Concentration dependence of **a** molecular weight, M_{wa}, and **b** hydrodynamic radius, R_h, of nanoparticles at 40 °C (procedure a); M_η= 122,000, c_{SR}/c_{PNIPA}=0.1

The Pluronic F68 concentrations used in the study are well below CMC; therefore, the behavior similar to systems with ionic surfactants should be observed. Instead, an intermediate behavior between the ionic and Brie surfactants was observed.

As to the dilution effect of SR/PNIPA solutions (at c_{SDS}/c_{PNIPA}=0.1) on M_{wa} and R_h of nanoparticles, the interpretation is more complicated. Both the phase transition kinetics and transport properties of surfactants slow down simultaneously on dilution. Therefore, a detailed explanation of the obtained results is impossible on the interpretation level used. Cooperative hydrophobic association of PNIPA polymer chains with ionic surfactant molecules [10, 13, 22, 26, 27] and subsequent formation of pearl necklace-like polymer-ionic surfactant complexes at surfactant concentrations lower than their CMC, which are formed below polymer phase transition, could be a reason for the observed decrease in both the M_w and R_h. These polymer-induced surfactant micelles increase the solubility of PNIPA on molecular level. Solubilization is more effective at higher concentrations and, therefore, M_{wa} and R_h decrease with increasing concentration. This solubilization effect is probably ineffective for nonionic surfactants having higher molecular weights than ionic ones. This could be a reason why the opposite behavior was observed.

Table 3 Characteristics of nanoparticles obtained from PNIPA of different molecular weights at 40 °C (procedure a); c_{PNIPA} = 5×10^{-4} and $c_{SR} = 5 \times 10^{-5}$ g · ml^{-1}

PNIPA $M_\eta \times 10^{-3}$	Nanoparticles $M_w \times 10^{-6}$	R_h (nm)	$\Delta R_h/R_h$
SDS [8]			
67	78	46.0	0.09
122	13	25.2	0.15
220	5.0	21.0	0.13
Pluronic F68			
67	1000	116	0.09
122	420	83.9	0.07
220	320	72.0	0.08
Brie 98			
67	8800	352	–
122	570	112	0.10
220	105	36.9	0.06

Conclusion

It was shown that well-defined thermoresponsive nanoparticles can be easily prepared by heating PNIPA solutions with low surfactant additions above the LCST. The nanoparticles are assumed to be monodisperse PNIPA nuclei formed at the early stage of phase separation stabilized by surfactants. A variety of surfactants, both ionic and nonionic ones, were tested. Varying chemical composition of surfactants, concentration of surfactants or PNIPA polymers and the molecular weight of PNIPA can change nanoparticle parameters in a wide range of M_w and R_h values.

The structure of particles is supposed to be similar to block copolymer micelles. Hydrophobic PNIPA molecules form the insoluble core of particles and their hydrophilic shell consists of hydrophilic parts of surfactants. An intermediate shell at the core–shell interface contains both the hydrophobic parts of surfactants and PNIPA chains. In our opinion, the nanoparticles covered with biocompatible poly(oxyethylene) shells seem to be good candidates for applications in biotechnology and in medicine.

Acknowledgment Financial support of the Grant Agency of the Academy of Sciences of the Czech Republic (grants A100500501) is gratefully acknowledged.

References

1. Hoffman AS (1997) Intelligent polymers. In: Park K (ed) Controlled drug delivery. ACS Publications, Washington, pp 485–502
2. Neony B, Kim SW, Bae YH (2002) Drug Deliv Rev 54:37
3. Oupický D, Diwadkar V (2003) Curr Opin Mol Ther 5:345
4. Taylor LD, Cerenkowski LD (1975) J Polym Sci 13:2551
5. Saiyto S, Konno M, Inomata H (1993) Adv Polym Sci 109:207
6. Wang X, Wu C (1999) Macromolecules 32:4299
7. Oupický D, Reschel T, Koňák Č, Oupická L (2003) Macromolecules 36:686
8. Koňák Č, Hrubý M (2006) Macromol Rapid Commun 27:877
9. Eliasaff J, Silberberg A (1959) J Polym Sci 41:33
10. Makhaeva EE, Tenhu H, Khokhlov AR (1998) Macromolecules 31:6112
11. Ricka J, Meewes M, Nyffenegger R, Binkert T (1990) Phys Rev Lett 65:657
12. Meewes M, Ricka J, de Silva M, Nyffenegger R, Binkert T (1991) Macromolecules 24:5811
13. Walter R, Ricka J, Quellet Ch, Nyffenegger R, Binkert T (1996) Macromolecules 29:4019
14. Wu C, Zhou S (1996) J Polym Sci, Part B: Polym Phys 34:1597
15. Hunter R (1987) Foundations of Colloid Science, Clarendon, Oxford, Chapter 10
16. Dautzenberg H, Rother G (1992) Makromol Chem, Macromol Symp 61:94
17. Dautzenberg H, Rother G (1998) J Polym Sci Part B: Polym Phys 26:353
18. Koňák Č, Reschel T, Oupický D, Ulbrich K (2002) Langmuir 18:8217
19. Jakeš J (1995) Collect Czechoslov Chem Commun 60:1781
20. Štěpánek P (1993) In: Brown W (ed) Dynamic light scattering. Clarendon, Oxford, pp 177
21. Heskins M, Guillet J (1968) J Macromol Sci Chem, Part A 2:1441
22. Schild HG, Tirrell D (1991) Langmuir 7:665
23. Schild HG, Tirrell D (1989) Polym Prepr 30:350
24. Cahn JW (1956) Acta Metall 4:449
25. Christian JW (1981) The theory of transformations in metals and alloys, Part I. Pergamon, New York
26. Dai S, Tam KC (2004) Langmuir 20:2177
27. Hsu Y-H, Chiang W-H, Chen M-C, Chern C-S, Chiu H-C (2006) Langmuir 22:6764
28. Kabir-ud-Din, Sinddiqui US, Kumar S, Dar AA (2006) Colloid Polym Sci 284:807
29. Koopal LK, Goloub TP, Davis TA (2004) J Colloid Interface Sci 275:360
30. Gente G, Iovina A, la Mesa C (2004) J Colloid Interface Sci 274:458